# Phases of carbon nanotube growth and population evolution from *in situ* Raman spectroscopy during chemical vapor deposition

Andrew Li-Pook-Than[1,2], Jacques Lefebvre[1], Paul Finnie[1,2,*]

* To whom correspondence should be addressed. E-mail: paul.finnie@nrc-cnrc.gc.ca

[1] Institute for Microstructural Sciences, National Research Council Canada

Building M-50,1200 Montreal Road, Ottawa, ON, K1A 0R6, Canada

[2]Department of Physics, University of Ottawa

150 Louis Pasteur, Ottawa, ON K1N 6N5, Canada

**Supporting information:**

*A. Changes to post-growth CNT Raman spectra with varying temperature:*

The spectral evolution of a Co sample initially grown and held at 800°C, before being cooled to progressively lower temperatures is presented in Fig. A1. At first, the analyzed RBM peaks will only slightly upshift ~3 $cm^{-1}$ with decreasing temperature, as expected; see, for example, the studies by Raravikar et al. and Uchida et al.[1, 2]. Below ~650°C, however, the notable disappearance of the RBM-1 and RBM-2 bands is typical and an expected consequence of the gradual shift in the Raman resonance condition with changing temperature. While only a few, weak RBMs are visible at high temperatures,

many RBMs are visible at low temperatures at higher intensity. On both sample types, the G band will tend to upshift with decreasing temperature by up to ~20 $cm^{-1}$ and the D band, when present, will tend to upshift by up to ~15 $cm^{-1}$. Below 200°C there is no significant change in any spectra. Finally, note that, while not fixed, the D/G ratio changes little with temperature, although the G and D-bands both become sharper at lower temperatures.

*B. Spectral background correction:*

The background correction was calculated similarly for all analyzed bands. As an example, Figure B1a depicts the RBM-1 and RBM-2 bands of the post-growth 813°C grown sample prior to cooling, while Figure B1b shows the corresponding G band. For a given peak, we measure where the band starts and ends within the Raman shift. We calculate an average intensity value at each end point by drawing a column about each end-point, measuring the integrated area beneath each end region, and dividing by the spectral width of the column. For RBMs, the column width is typically ~7 $cm^{-1}$, while for the G and D bands it is typically ~31 $cm^{-1}$. We can now draw a line between these two averaged end intensities and subtract away the trapezoidal background area that lies beneath it (in blue), leaving the corrected Raman area (in red). Depending on the shape of the spectral background and the signal/noise ratio of the peak, a constant may be added or subtracted to ensure a pre-growth area of 0.

*C. Waterfall plots:*

The growth evolution, Raman area traces of the G band, D band, RBM-1 bands and RBM-2 bands for the Co sample are presented in Figures C1-C4, respectively, as a function of temperature. Likewise, the G band and D band traces for the Co-alumina samples are presented in Figure C5-C6, respectively. N.B. For the Co sample grown at 850°C, a 4.5s exposure time was used instead of the usual 5s.

*D. Fitting the evolution curves:*

The fitting of the G band time evolution data for the 850°C grown Co sample is shown as an example in Figure D1. There is a finite travel time for gas to reach the chamber, and we attribute the first 30 seconds to this travel time.

After this time, the Raman signal intensity remains zero for an additional time, which is temperature dependent. The duration of this stage we call "incubation" (in blue) is determined by subtracting the 30s travel time from the time at which the Raman signal is just noticeably non-zero. This is determined by eye. In this case, this duration $t_{inc}$ = 90s ± 20s.

The accelerating stage is fit (in orange) to $I = A_0 \exp(t/\tau_{acc})$, where I is the integrated intensity of the Raman band. $A_0$ is related the nanotube yield, t is the time, as measured from end of the incubation, and $\tau_{acc}$ is the characteristic time of the exponential. In this case, $\tau_{acc}$ = 32s ± 11s. In order to estimate the uncertainty, several fits are performed using different starting times and end times to see how much the characteristic

time varies.

The linear growth stage duration is estimated by determining the range over which a straight line fit is reasonable. The uncertainty is estimated by trying different fits. In this case the duration of the linear stage is $t_{lin}$ = 130s ± 30s. It is verified by a linear fit (in green).

The termination stage is fit (in red) to $I = I_0 - A_0 \exp(t - t_0/\tau_{term})$, where $\tau_{term}$ is the associated characteristic time (i.e. $\tau_{term}$ = 139s ± 55s) and $I_0$ is the intensity offset. Many fits using different origins for the exponential are taken to estimate the uncertainty. In some cases, such as the one shown here, the signal continues to increase slowly and near linearly for a long time. This long, slow change was not fit.

A fit of another G band data set is shown in Figure D2. This is the evolution data for the 725°C grown Co sample. The result of this fit is an incubation time shorter than the time resolution, $\tau_{acc}$ = 11s ± 4s, $t_{lin}$ = 15s ± 5s, and $\tau_{term}$ = 33s ± 10s. In this case, the curve is almost flat, showing little evolution after the exponential termination.

*E. Characteristic energy plots with additional RBM-1 and D band data:*

Figure E1 is identical with Figure 5, except that the Co samples' RBM-1 band incubation times, in addition to the Co-alumina samples' D band incubation and acceleration times, have been added. All other band data is too weak to extract meaningful values. These additional RBM-1 incubation times and the D band acceleration times closely match their corresponding G band values. The characteristic energy plots for the Co incubation times and the Co-alumina acceleration times have also

been re-plotted by combining the corresponding new data with G band data on each sample type, and new characteristic energies agree with the original values obtained from Figure 5. The D band incubation times are difficult to measure at higher temperatures due to the low D total D band intensity as well as the broadening at high temperature. It is unclear in the high temperature regime whether the actual D band onset lags behind that of the G band, or whether the D band onset is the same as the G band, but is buried in the noise.

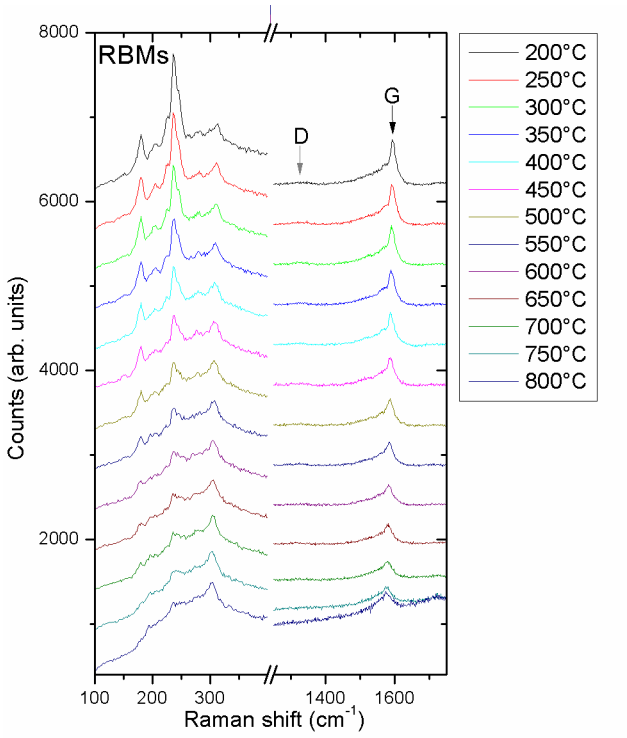


Figure A1: Post-growth Co Raman spectra for sample grown at 800°C at different temperatures. As temperature is decreased from 800°C, RBMs become stronger and more distinct, while many RBMs emerge. The G band becomes distinct with clear G+ and G- areas at low temperature. However, its integrated intensity is relatively unchanged.

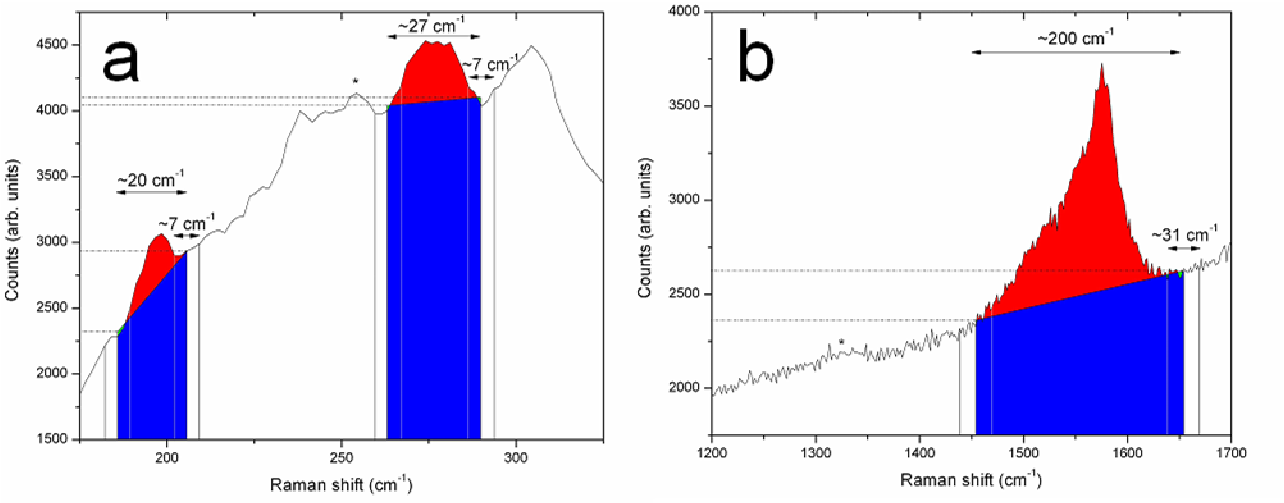


Figure B1. Background correction performed on spectra from the post-growth 813°C grown Co sample taken at 813°C for the (a) RBM-1 and RBM-2 bands and (b) the G band. Red areas indicate the corrected band intensity, while blue regions indicate the background. Asterisks indicate Raman bands that are too weak to use to extract trends.

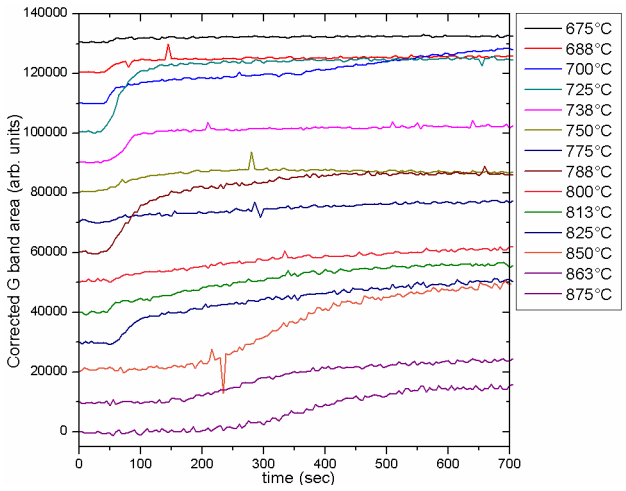


Figure C1: Waterfall plot of corrected Raman intensity growth evolution for the G-band of Co samples grown at different temperatures. All Co samples had G band intensities sufficiently strong enough to track at their corresponding growth temperatures.

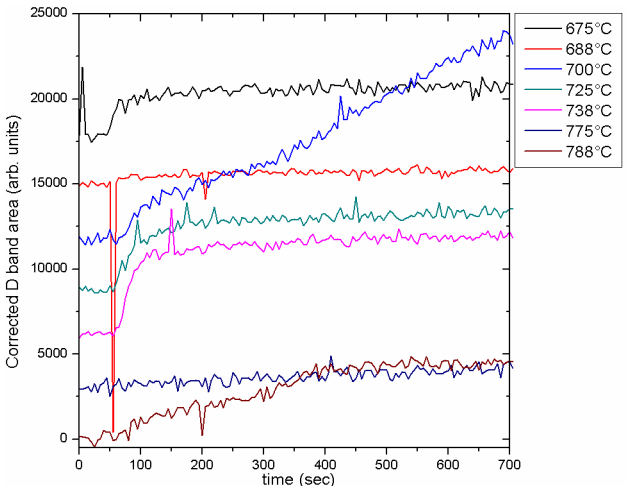


Figure C2: Waterfall plot of corrected Raman intensity growth evolution for the D-band of Co samples grown at different temperatures. Omitted samples had D-band intensities too low to track at high temperature.

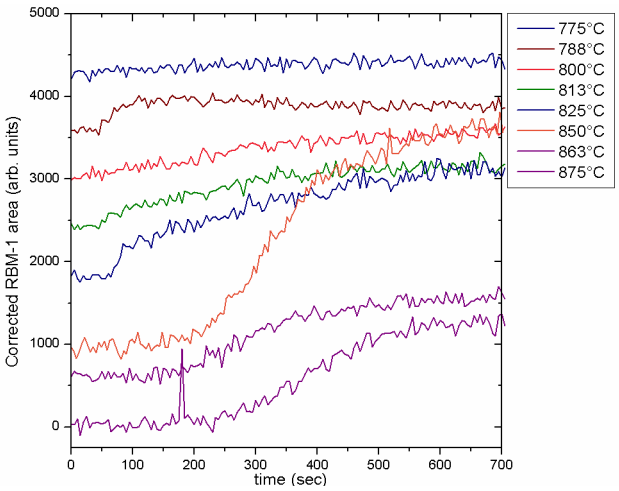


Figure C3: Waterfall plot of corrected Raman intensity growth evolution for the RBM-1 of Co samples grown at different temperatures. Omitted samples had RBM-1 intensities too low to track at high temperature.

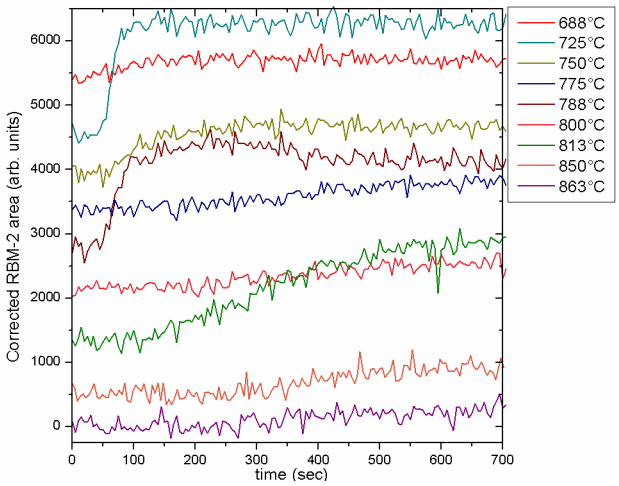


Figure C4: Waterfall plot of corrected Raman intensity growth evolution for the RBM-2 of Co samples grown at different temperatures. Omitted samples had RBM-2 intensities too low to track at high temperature.

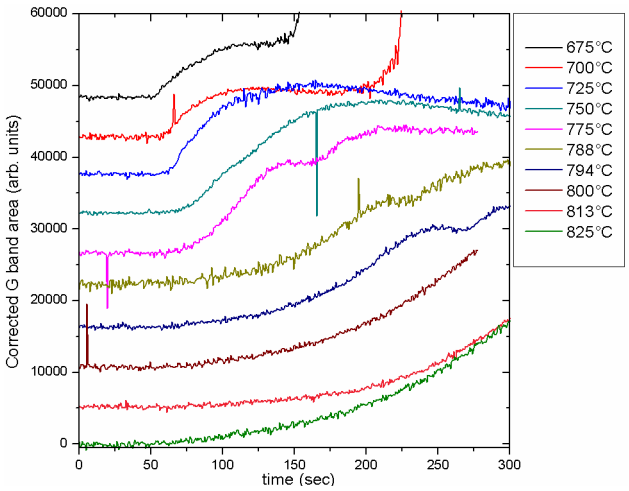


Figure C5: Waterfall plot of corrected Raman intensity growth evolution for the G-band of Co-alumina samples grown at different temperatures. All Co-alumina samples had G-band intensities sufficiently strong enough to track at their corresponding growth temperatures. The dips/sudden jumps in the extracted G band signals occur when the nanotube film has become too thick and opaque, and show when the Raman signal is no longer a good indicator for the amount of nanotube growth.

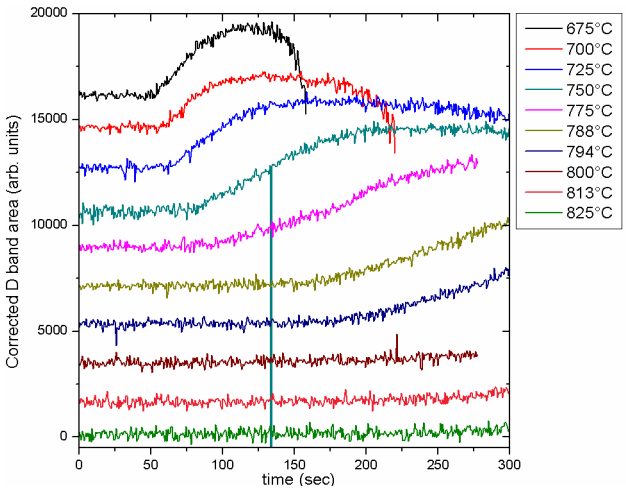


Figure C6: Waterfall plot of corrected Raman intensity growth evolution for the D-band of Co-alumina samples grown at different temperatures. Omitted samples had D-band intensities too low to track at high temperature. The dips in the extracted D band signals occur when the nanotube film has become too thick and opaque, and show when the Raman signal is no longer a good indicator for the amount of nanotube growth. The 675°C and 700°C evolution plots are clipped at large time values.

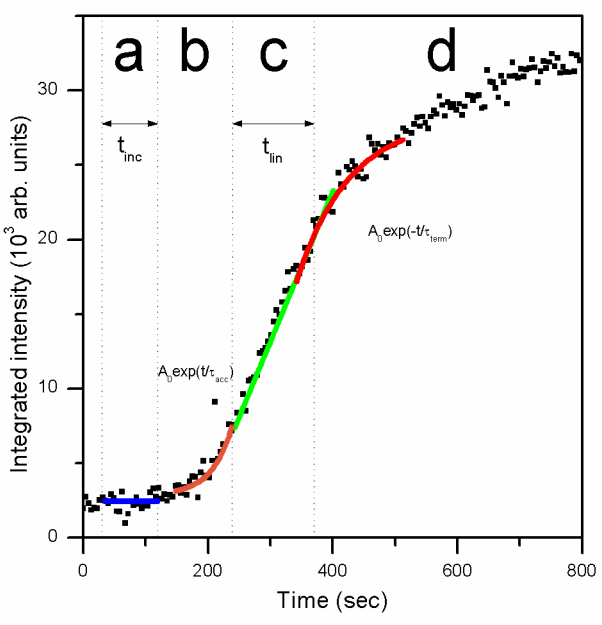


Figure D1: Kinetic curve fitting of the 850°C grown Co sample G band evolution data for the (a) incubation, (b) accelerating, (c) linear, and (d) termination growth phases shown respectively in blue, orange, green, and red.

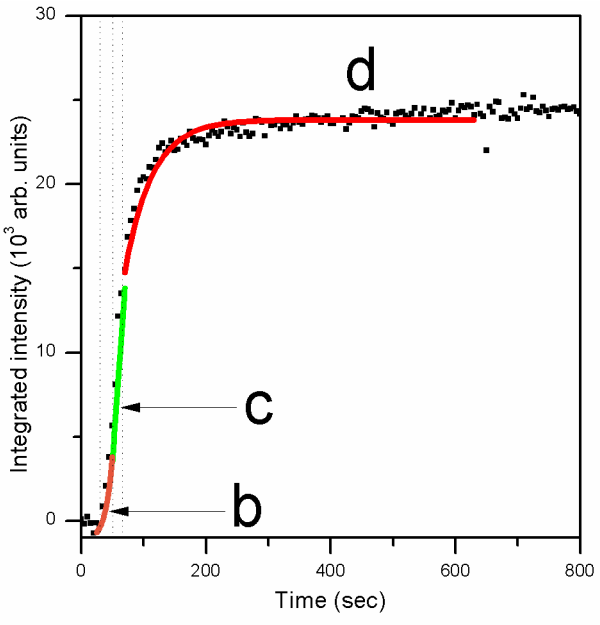


Figure D2: Kinetic curve fitting of the 725°C grown Co sample G band evolution data for the (b) accelerating, (c) linear, and (d) termination growth phases shown respectively in orange, green, and red. The duration of the (a) incubation phase is 0s.

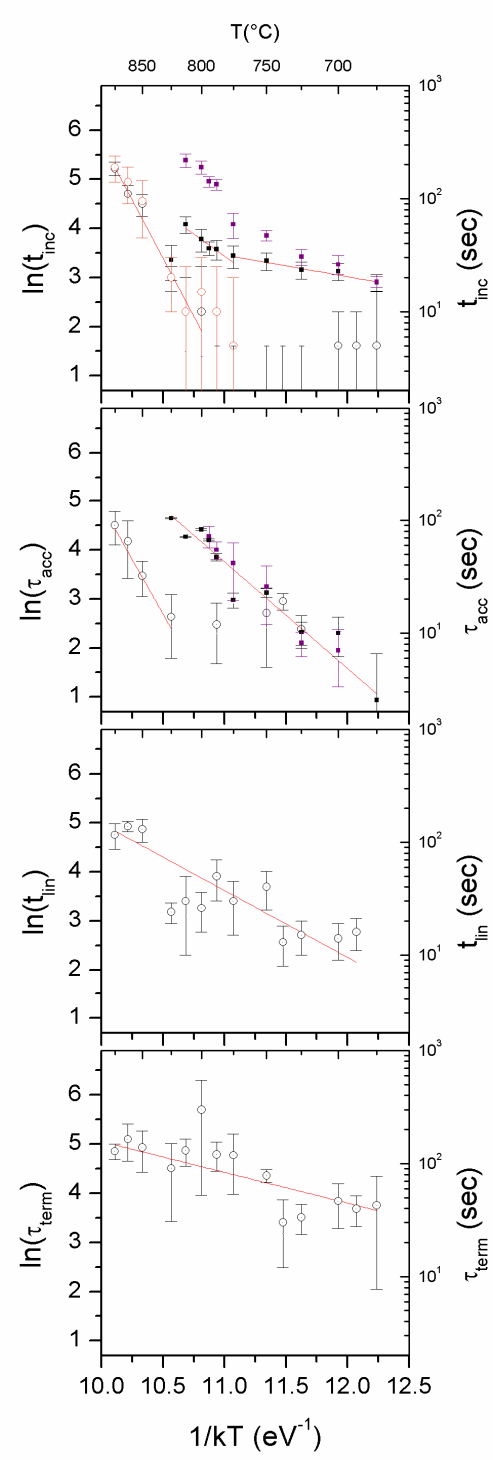


Figure E1: Characteristic energy plots of the Co and Co-alumina time constants: (a) incubation time; (b) accelerating time; (c) linear time; (d) termination time. Co-alumina linear and termination time constants could not be obtained. Characteristic times from the

integrated G band intensity for the Co (white circles) and Co-alumina (black squares) samples and from the corresponding Co RBM-1 bands (orange circles) and Co-alumina D bands (violet squares) are plotted. Characteristic energies correspond to the slope of the linear plots (red lines).

**References**

(1) Raravikar, N. R.; Keblinski, P.; Rao, A. M.; Dresselhaus, M. S.; Schadler, L. S.; Ajayan, P. M. Temperature Dependence of Radial Breathing Mode Raman Frequency of Single-Walled Carbon Nanotubes. *Phys. Rev. B* **2002**, *66*, 235424.

(2) Uchida, T.; Tazawa, M.; Sakai, H.; Yamazaki, A.; Kobayashi, Y. Radial Breathing Modes of Single-Walled Carbon Nanotubes in Resonance Raman Spectra at High Temperature and their Chiral Index Assignment. *Appl. Surf. Sci.* **2008**, *254*, 7591-7595.